

# Performance analysis for parallel operation of multimode droop controller doubly fed induction generator based wind energy conversion system with other wind unit, solar unit, loads, and FACTS device

Kelothu Naresh<sup>1</sup>, Puthireddy Umapathi Reddy<sup>2</sup>, Peddakotla Sujatha<sup>1</sup>

<sup>1</sup>Department of Electrical and Electronics Engineering, Jawaharlal Nehru Technological University Hyderabad, Hyderabad, India

<sup>2</sup>Department of Electrical and Electronics Engineering, Sree Vidyanikethan Engineering College, Tirupati, India

## Article Info

### Article history:

Received May 29, 2023

Revised Sep 18, 2024

Accepted Oct 19, 2024

### Keywords:

DFIG

Grid connected mode

Islanded mode

Multimode strategy

Solar unit

## ABSTRACT

Due to its numerous advantages, wind turbines with changeable speed power production systems are increasingly being used. This study proposes the architecture and specifications of an induction turbine generating wind system, as well as PI controller-based DC voltage link regulator and optimal torque control system. The suggested control technique as stated in this paper allows the system to function in grid linked mode as well as islanded mode and also in parallel with other power generation units, loads, FACTS devices, etc. This paper involves the analysis of different test cases in grid connected mode as well as islanded mode with PV generation unit, passive loads, induction motor loads, other wind energy generation systems. The paper also includes the analysis of response of the system with the switching on and off of the other units. MATLAB 2013a thereby validates the system findings and analysis.

*This is an open access article under the [CC BY-SA](https://creativecommons.org/licenses/by-sa/4.0/) license.*



## Corresponding Author:

Kelothu Naresh,

Department of Electrical and Electronics Engineering, Jawaharlal Nehru Technological University

Sir Mokshagundam Vishveshwariah Road, Ananthapuramu, Andhra Pradesh 515002, India

Email: naresh5kelothu@gmail.com

## 1. INTRODUCTION

From the last few years there have been number of disturbances occurring in the power system like power quality problems, power shut down problems. So there has to be a solution to reduce these problems using renewable energy sources for effective, efficient eradication of environmental issues, continuity of power supply. Wind energy and solar energy are considered as sources for power generation among the numerous sources as they are unlimited supply of source, environmental friendly [1], [2]. But the disadvantage of the two renewable energy sources is may not be available all the day. So, continuity of power supply can be a problem and so there is a necessity of the storage elements. Also, there number of energy storage devices like superconductive magnetic energy storage (SMES), flywheels, and uninterruptible power supply (UPS) [3]–[6]. But due to cost issue problems DC link capacitor and battery has been considered as energy storage devices. There may not be necessity or requirement for the grid integration all the time, so a controller for controlling the wind energy source is required for effective system operations in grid connected mode or in islanded as per the requirement [7], [8]. Solar system has been integrated at the system's point of common connection as an alternative renewable energy source. The system is also integrated with other RL load, induction motor load which can also be simultaneously operated representing parallel loads operation. The system is also designed to working connection with the fixed speed wind energy systems [9]–[11]. There may be abnormal power

quality problems within the grid connection and to ensure the proper operation, flexible AC transmission system (FACTS) device is also integrated at the common coupling point.

This study comprises the diagram of a wind turbine of variable speed with a multimode core strategy and the analysis of the proposed system's operation using different test scenarios to guarantee the proposed system's efficient performance under both normal and faulted scenarios [12]–[14]. The study is organized as: the first section makes an introduction of the proposed system, whereas the second section delves into the block diagram explanation of the suggested developed framework with parallel units and their computational analysis. In addition, section 3 is devoted to discussing simulation efforts as well as outcomes. The fourth section is critical at discussing the results obtained from the work [15].

## 2. A BLOCK MODEL AND MATHEMATICAL MODELLING OF PREFERRED SYSTEM

Figure 1 highlights the diagram of the block model. The model contains doubly-fed induction generator (DFIG) based wind unit, permanent magnet synchronous generator (PMSG) based wind unit, statcom FACTS device, and induction generator-based wind generation unit, solar generation unit, RL load and induction motor load [16]–[19]. The system is designed to enhance the comparable operated grid connected systems. It can be run in grid-connected technique or islanded technique with the disconnection of grid. All the parallel units are grouped into a single coupling point so the continuity of grid operation can be obtained with enabling any generation unit without any interruptions [20], [21]. All the units are connected through the three phase breakers at the common coupling point. Moreover, it can be operated under faulted conditions due to the connection of FACTS devices or other parallel units [22]–[26].

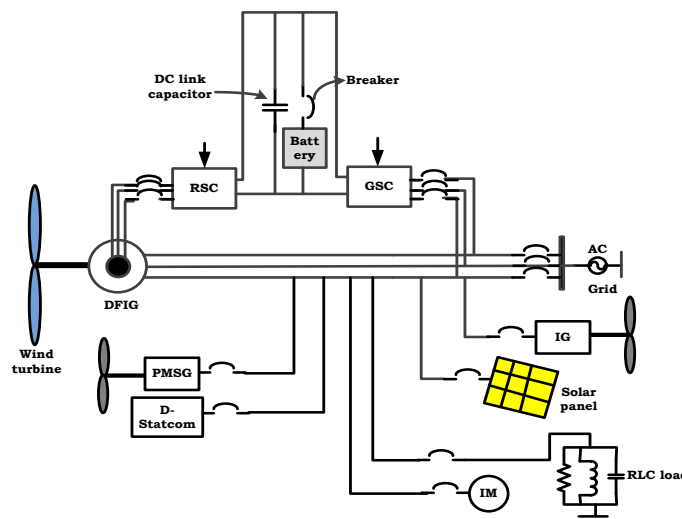


Figure 1. A block model of suggested system with parallel units

### 2.1. DFIG based wind generation unit

The DFIG based wind generation unit comprises of a wind generator for trying to convert wind energy into mechanical energy, an induction generator (DFIG generator) for transforming mechanical power into electricity, whose stator windings are actively connected to the utility grid, consecutively connected two voltage source converters (VSC) used to connect the DFIG's propellers to the grid, a DC converter capacitor and a battery are the energy storage elements connected in between the converters to store the energy to provide uninterruptible power supply [27]–[29]. The advantages of DFIG based wind generation unit are availability of variable speed operation there by full range of speed, power control, bidirectional power supply. The DFIG system also employs two controllers for the two VSC's for the droop control of system frequency, voltage, real, and reactive power [30], [31].

#### 2.1.1. DFIG equivalent circuit

The DFIG constitutes of both rotor and stator windings whose parallel circuit is illustrated in Figure 2 containing rotor, stator resistance and inductances, voltages at the rotor and stator windings are represented with their sources of voltage power.

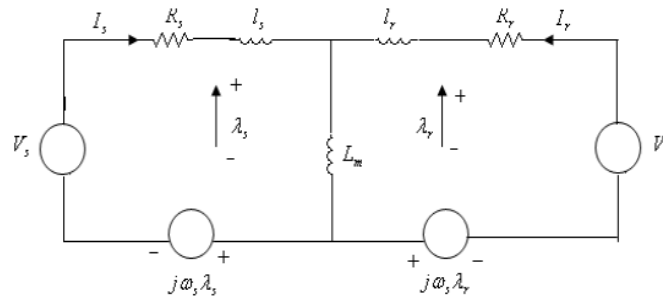


Figure 2. Analogous circuit of DFIG

Below are the dynamical equations representing the equivalent circuit (1) and (2):

$$V_s = I_s R_s + j\omega_s L_s I_s + j\omega_s m I_r \tag{1}$$

$$V_r = I_r R_r + j\omega_s L_r I_r + j\omega_s m I_s \tag{2}$$

the power flow equations can be given as:

$$P_m = T_m \omega_r \tag{3}$$

$$P_s = T_e \omega_s \tag{4}$$

the expression for the mechanical torque and electro- magnetic torque can be given as (5).

$$T_m = J \frac{d\omega_r}{dt} + D\omega_r + T_e \tag{5}$$

Assuming the rotational and friction losses are negligible, then the above equation becomes:

$$T_m - T_e = J \frac{d\omega_r}{dt} \tag{6}$$

assuming the generator is loss less:

$$T_m = T_e \tag{7}$$

$$P_m = P_s + P_r \tag{8}$$

**2.1.2. Droop based method**

The droop-based method is based on the relationship between voltage, power and frequency and their regulation. It determines the variation of real, reactive power in relation to voltage and frequency. The following are the equations relating the voltage, power and frequency. Representation of transmission line shown in Figure 3 and their droop characteristics shown in Figure 4 (a) frequency droop and (b) voltage droop characteristics.

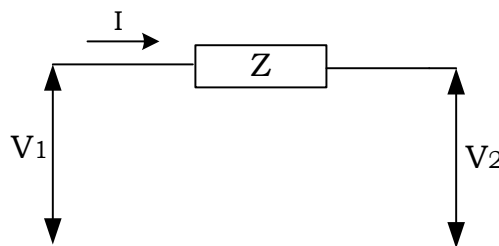


Figure 3. Representation of transmission line

The equation relating active power and voltage of a line can be given as (9).

$$P = \frac{V_1^2}{Z} \cos\theta - \frac{V_1 V_2}{Z} \cos(\theta + \delta) \quad (9)$$

The equation relating reactive power and voltage of a line can be given as (10) to (12),

$$Q = \frac{V_1^2}{Z} \sin\theta - \frac{V_1 V_2}{Z} \sin(\theta + \delta) \quad (10)$$

$$\delta = \frac{XP}{V_1 V_2} \quad (11)$$

$$V_1 - V_2 = \frac{XQ}{V_1} \quad (12)$$

the equation linking with the active power and frequency of a line with a gain of  $k_p$  is as (13) and (14),

$$f - f_0 = k_p(P - P_0) \quad (13)$$

$$V - V_0 = k_Q(Q - Q_0) \quad (14)$$



Figure 4. Droop characteristic of transmission line, (a) frequency droop and (b) voltage droop characteristics

### 2.1.3. Rotor side controller (RSC)

The expression for torque in terms of the above-mentioned equivalent circuit can be given as (15) and (16)

$$i_{dr-ref} = \frac{\omega_s(L_s + L_m)}{L_m V_{ds}} T_{e-ref} \quad (15)$$

$$Q = \left( \frac{V_{ds}^2}{\omega_s(L_m + L_s)} + \frac{V_{ds} L_m i_{qr}}{(L_s + L_m)} \right) \quad (16)$$

#### a. Active power controller

Wind energy that was drawn is as (17),

$$P = \frac{1}{2} \rho A V^3 C_p \quad (17)$$

(17) can be modified as (18).

$$P = K \omega_r^3 \quad (18)$$

Based on the power-torque relation, the expression for the torque can be obtained from the power equation and can be given as (19).

$$T = K \omega_r^2 \quad (19)$$

From (19) it can be concluded that controlling torque, speed, and active power can be done with the rotor side controller [32]–[35].

**b. Current controller**

Based on the torque and current measurements, the q and d axes are calculated and then processed through the controllers to produce d and q axes voltages to generate gating pulses for rotor side converter. A model representation of current controller is shown in Figure 5.

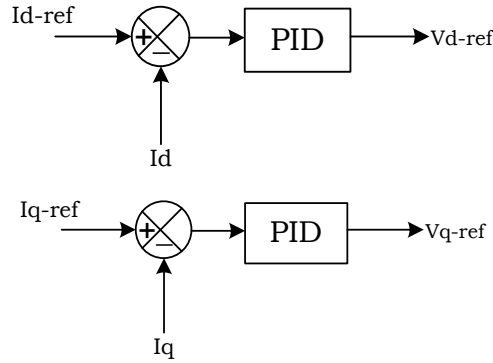


Figure 5. A model representation of current controller

**2.1.4. Grid side controller (GSC)**

**a. Active power controller**

The DC link voltage is connected between the GSC and RSC converters. The power from the grid side is measured by altering the DC voltage, as shown in (20). The current controlling is also performed with the DC link as shown in Figure 6.

$$P_{rsc} - P_{gsc} = \frac{1}{2} C \frac{d}{dt} (V_{dc}^2) \tag{20}$$

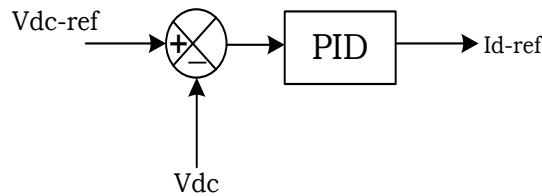


Figure 6. DC link voltage controller

**2.1.5. Control of the pitch angle**

This has also been performed in the proposed system to control the angle of the blades there by running the power according to the low speed and high wind speeds.

**2.2. PMSG wind generation unit and IG based wind generation**

The two parallel wind power generation units that are linked at the common coupling point includes: varying wind power speed generation system and wind energy generation system within the limited range. The fixed speed wind generation unit employs the PMSG and wind energy is shown in Figure 7. The induction squirrel cage power supply (IG) and wind energy are used in the variable speed generation unit. The energy transmitted is same as the DFIG wind generation unit but the disparity is there is no bidirectional power flow and these are intertwined directly to the grid without side-to-side connection. Also, no controlling strategy has been employed for these generation units as these are back up devices.

**2.3. Solar power generation unit**

Solar power is one of the efficient sustainable resources utilizing sun rays to produce electrical energy. The proposed solar power generation unit consists of solar panel, boost converter, power tracker, as well as three phase inverters. A solar panel was created by connecting numerous solar panels in parallel and series

configurations. The circuit model for a solar array is shown in Figure 8, which contains a diode, current source, and series and parallel impedances.

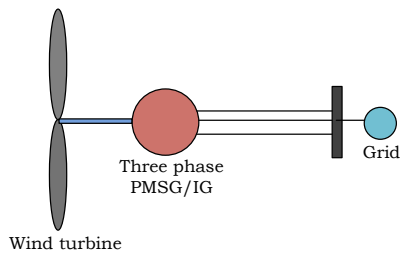


Figure 7. Block representation of PMSG based wind generators

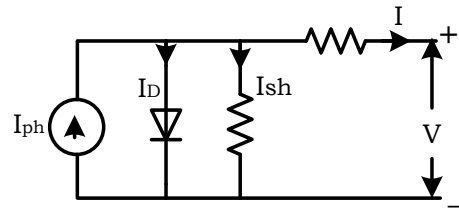


Figure 8. Comparable circuit for a solar cell

The following is the formula for the power generated by the solar cell:

$$I = I_{ph} - I_D - I_{sh} \tag{21}$$

the input power that flows through the diode is denoted by (22).

$$I_D = I_0 \left[ e^{q \left( \frac{V+IR_S}{AKT} \right)} - 1 \right] \tag{22}$$

The voltage passing through the resistance value is denoted as:

$$I_{sh} = \frac{V+IR_S}{R_{sh}} \tag{23}$$

**2.4. STATCOM**

These days there are frequent disturbances like voltage drops, transients, fluctuations occurring in the power system. So, to provide ripple free and disturbance free supply compensation of the reactive power has to be done which can be efficiently performed by the FACTS devices. Among the number of available FACTS devices, distribution static compensator (D-STATCOM) has been chosen in the proposed work due to its advantages like less expensive, less maintenance, effective in compensating line voltage harmonics.

D-STATCOM is a voltage source converter with output current designed with GTO or IGBT which is fuelled by batteries or capacitors and is linked to the network in parallel via a coupling capacitor as shown in Figure 9(a). It generates alternating voltage thee by changing the reactive power with the change of gate pulse of voltage source converter. The D-STATCOM output voltage ( $V_{sh}$ ) is adjusted in sync with the voltage level ( $V_t$ ), and the voltage fluctuates with the voltage. If  $V_t < V_{sh}$ , voltage is leading the output voltage,  $V_t > V_{sh}$ , voltage is lagging the output voltage and if  $V_t = V_{sh}$ , no dynamic current is transmitted to the network. Analogy circuit of D-STATCOM is shown in Figure 9(b).

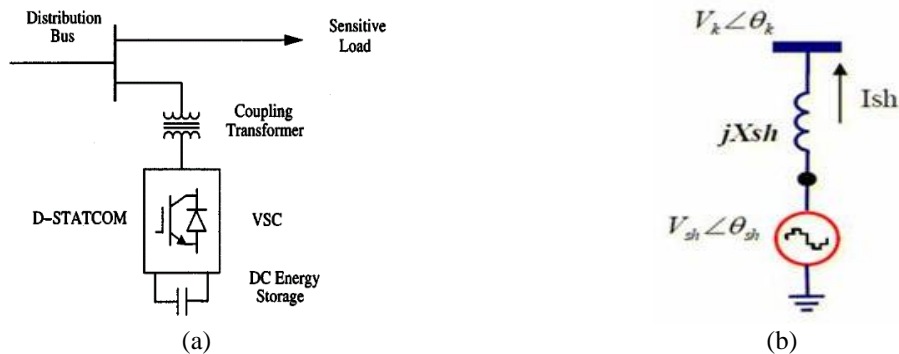


Figure 9. These figures are; (a) structure of D-STATCOM and (b) analogy circuit of D-STATCOM

The equations defining active power, reactive power of the network is given as (24) and (25)

$$P = \frac{V_s V_{sh}}{X_t} \sin \delta_{sh} \tag{24}$$

$$Q = \frac{V_s^2}{X_t} - \frac{V_s V_{sh}}{X_t} \cos \delta_{sh} \tag{25}$$

**2.5. RL load and induction motor load**

Another test case has been conducted for the proposed system with the connection of parallel RL load and a three-phase induction motor. An RL load can be operated with the utilization of supply at the point of common coupling.

**3. SIMULATION RESULTS**

**3.1. Test 1: when the operating system (OS) is grid-connected with a battery**

The waveforms of voltage of the DC link are shown in Figure 10(a). Battery power is shown in Figure 10(b). Frequency is shown in Figure 10(c) and speed when running the system in grid mode is shown in Figure 10(d).

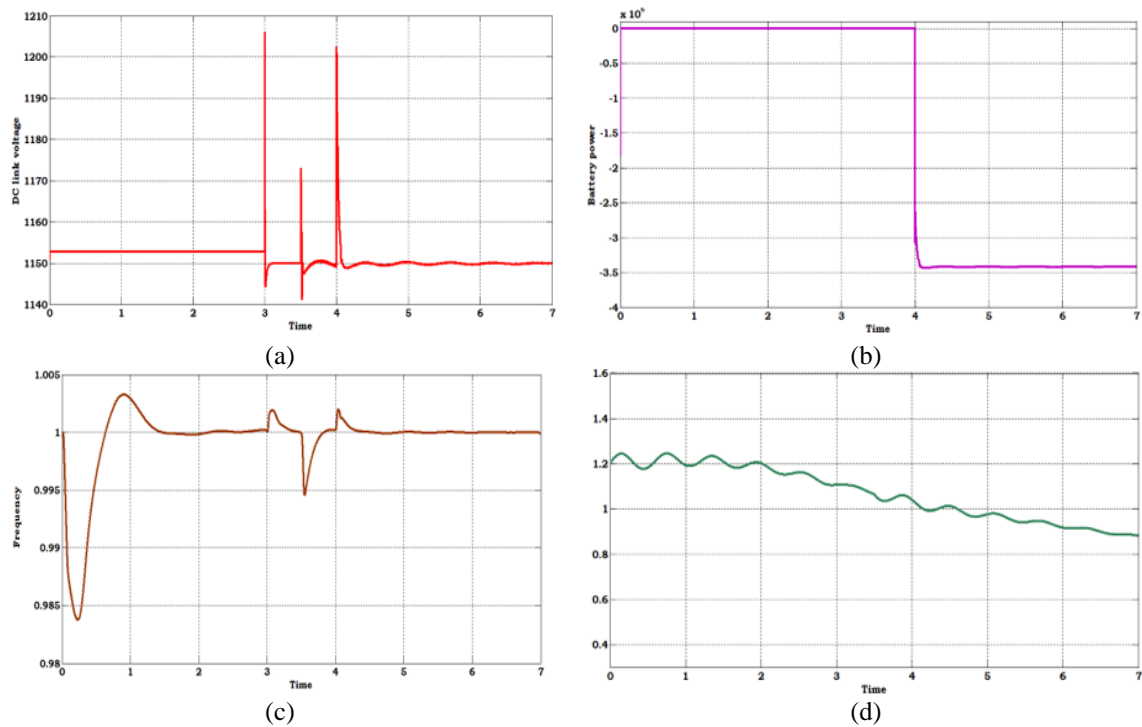


Figure 10. The waveforms of (a) voltage of the DC link, (b) power from a battery, (c) frequency, and (d) speed when running the system in grid mode

It is activated during system start up from t=0 to t=7 s. From t=0 to t=7 s, a wind velocity of 10 m/s is sent to the rotor. The DC connection is kept at the initial capacitor voltage value from t=0 to t=3 s. At t=3 s, the GSC breaker is activated, followed by a fluctuation in the output, after which the DC voltage controller switches on and conserves the amplitude and current at the value of reference. The circuit at RSC is activated at t=3.5 s, and the battery is closed from t=4 s to t=7 s, indicating that the controllers are tracking continuously by keeping the speed, frequency, and DC connection current constant.

**3.2. Test 2: when the OS is connected with the grid and the battery is suddenly disconnected**

The waveforms of Voltage of the DC link are shown in Figure 11(a). Battery power is shown in Figure 11(b). Frequency is shown in Figure 11(c) and when the system is linked with the grid and the battery is suddenly disconnected, the speed is increased as shown in Figure 11(d).

When the system is linked with the grid and the battery is suddenly disconnected, the speed is increased. This configuration is similar as the start-up scenario from  $t=0$  s to  $t=4$  s, and at  $t=4$  s, the charger is abruptly disengaged from the mechanism, with the strength of the power supply depicted in the under start figuring being lowered to a negative figure, indicating that the power supply is accessible and thus no transmission of power, but the link voltage is monitored by the controller, and bandwidth control is also performed.

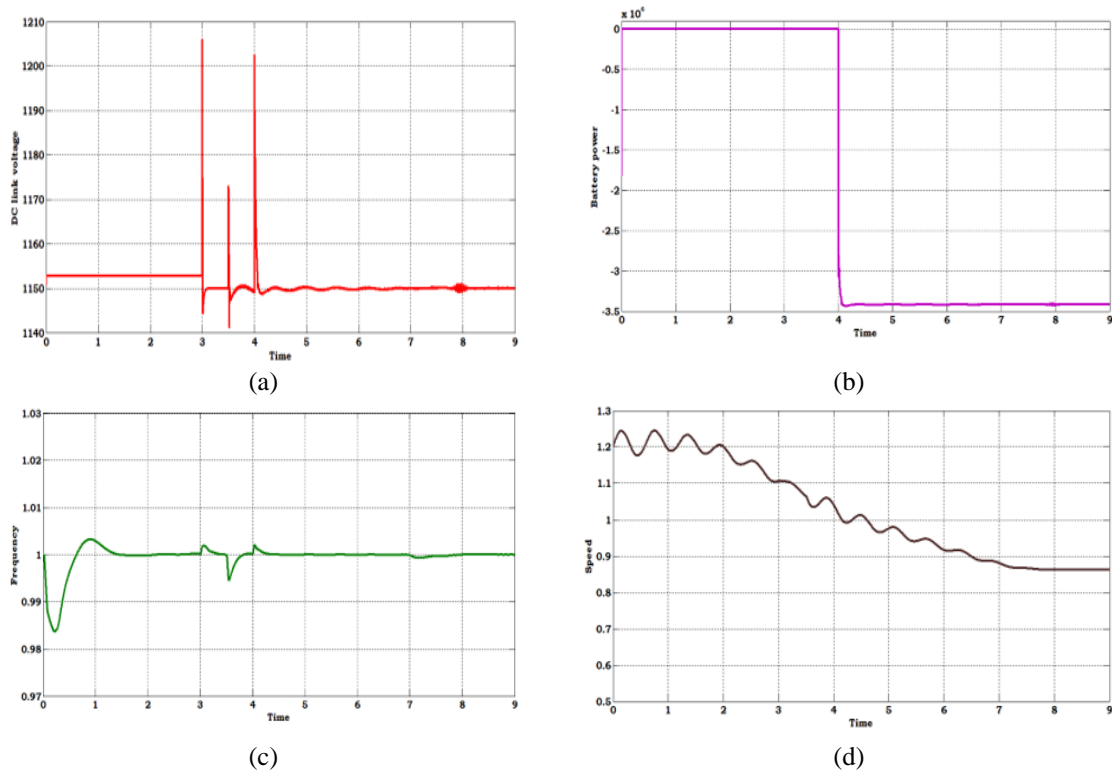


Figure 11. The waveforms of (a) voltage of the DC link, (b) power from a battery, (c) frequency, and (d) speed

### 3.3. Test 3: when the OS is in grid connected mode and other units connect suddenly ( $t=0$ to $t=15$ s)

Waveforms of link voltage, battery energy, converter's active current, converter's reactive energy, frequency, pitch angle, power generated, power transmitted and speed are shown in Figures 12(a) to 12(i).

This mode is same as the start up case from  $t=0$ , to  $t=7$  s. At  $t=7$  s, RL load and induction motor loads are tuned ON and turned OFF at  $t=8$  s. In the same manner other wind units, PV system, D-STATCOM are turned on at  $t=9$  s,  $t=11$  s,  $t=13$  s. The below waveforms show that the controlling is performed all the time but the turning ON the PV, FACTS device injects huge amount of voltage, power.

### 3.4. Test 4: when OS is connected in grid with instant fault

It is same as the initial case from  $t=0$  s to  $t=7$  s and at  $t=7$  s, three phase fault has been created at the common coupling point to ensure the controlling which is shown in Figure 13. Waveforms of DC link voltage, Battery power, frequency and power transmitted are shown in Figures 13(a) to 13(d).

### 3.5. Test 5: when the OS in an islanded manner

This mode is same as the start up case from  $t=0$  s to  $t=7$  s and at  $t=7$  s, the grid is suddenly isolated from the system where the power transmitted or at the common coupling point is reduced to zero but all the parameters of the DFIG are simultaneously controlled. The waveforms of voltage of the DC link, power from a battery, converter active power, converter reactive power, frequency, angle of pitch, transmission of power and when the OS is in islanded mode, the speed increases are shown in Figures 14(a) to 14(h).



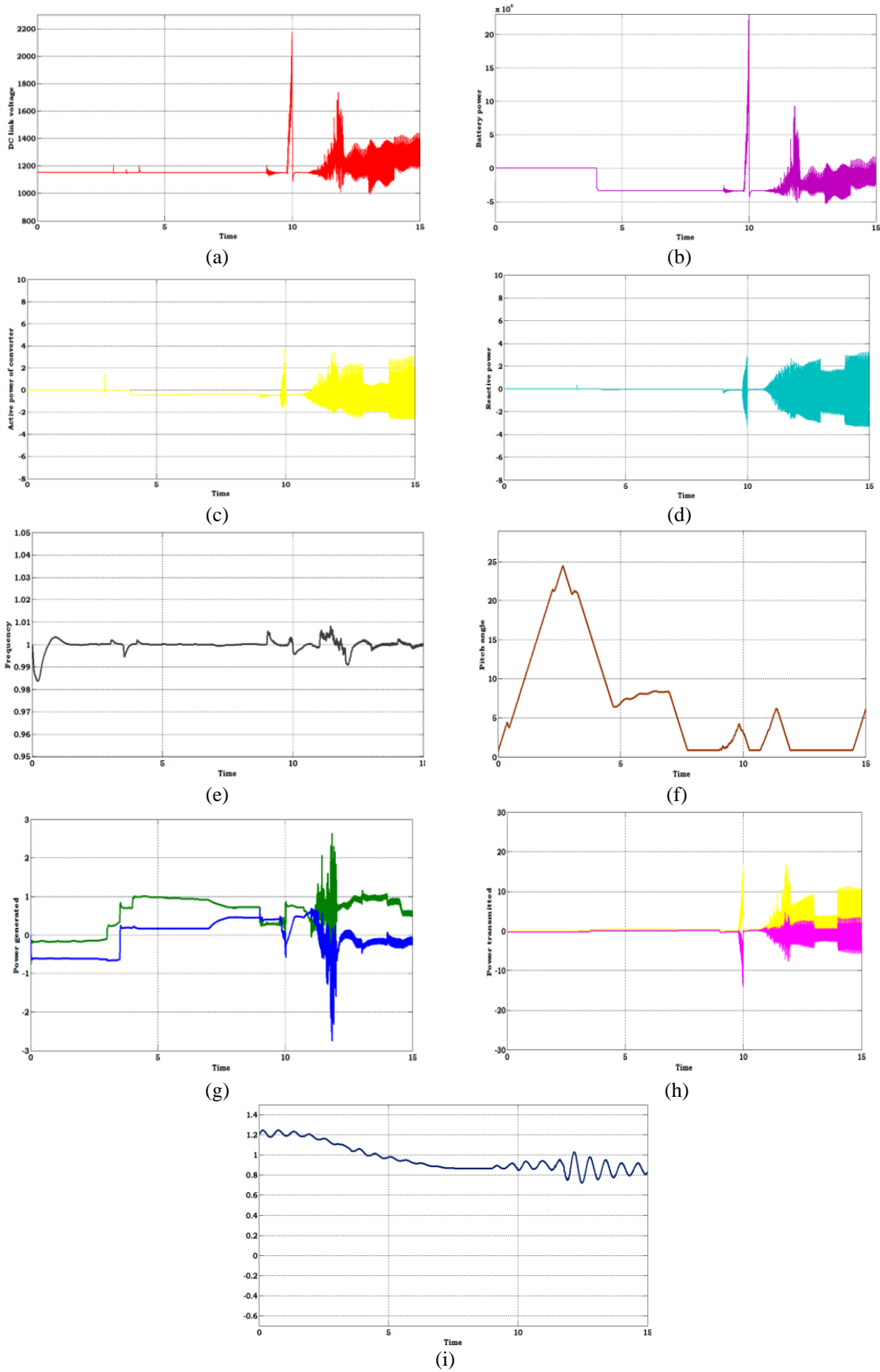


Figure 12. Waveforms of (a) link voltage, (b) battery energy, (c) converter's active current, (d) converter's reactive energy, (e) frequency, (f) pitch angle, (g) power generated, (h) power transmitted, and (i) speed

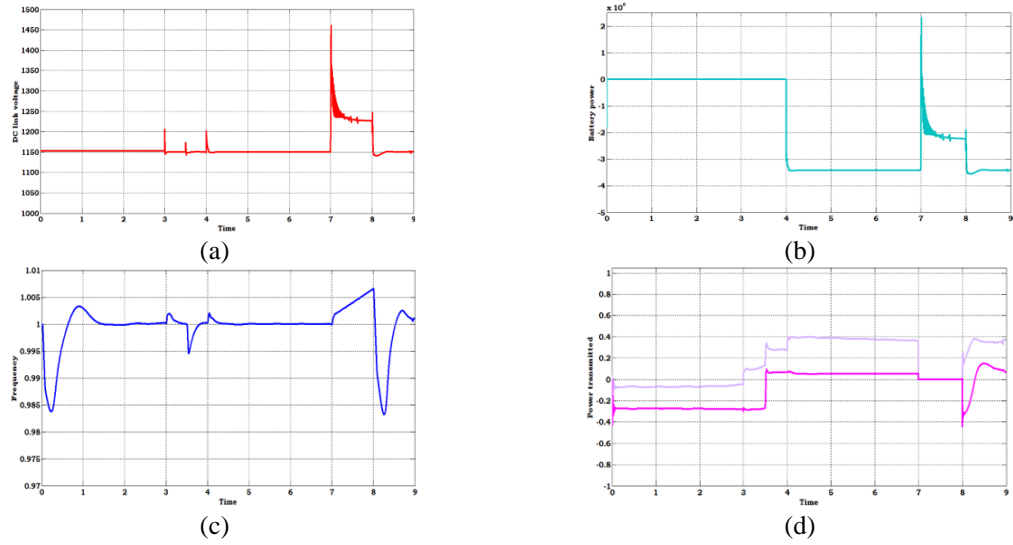


Figure 13. Waveforms of (a) DC link voltage, (b) battery power, (c) frequency, and (d) power transmitted

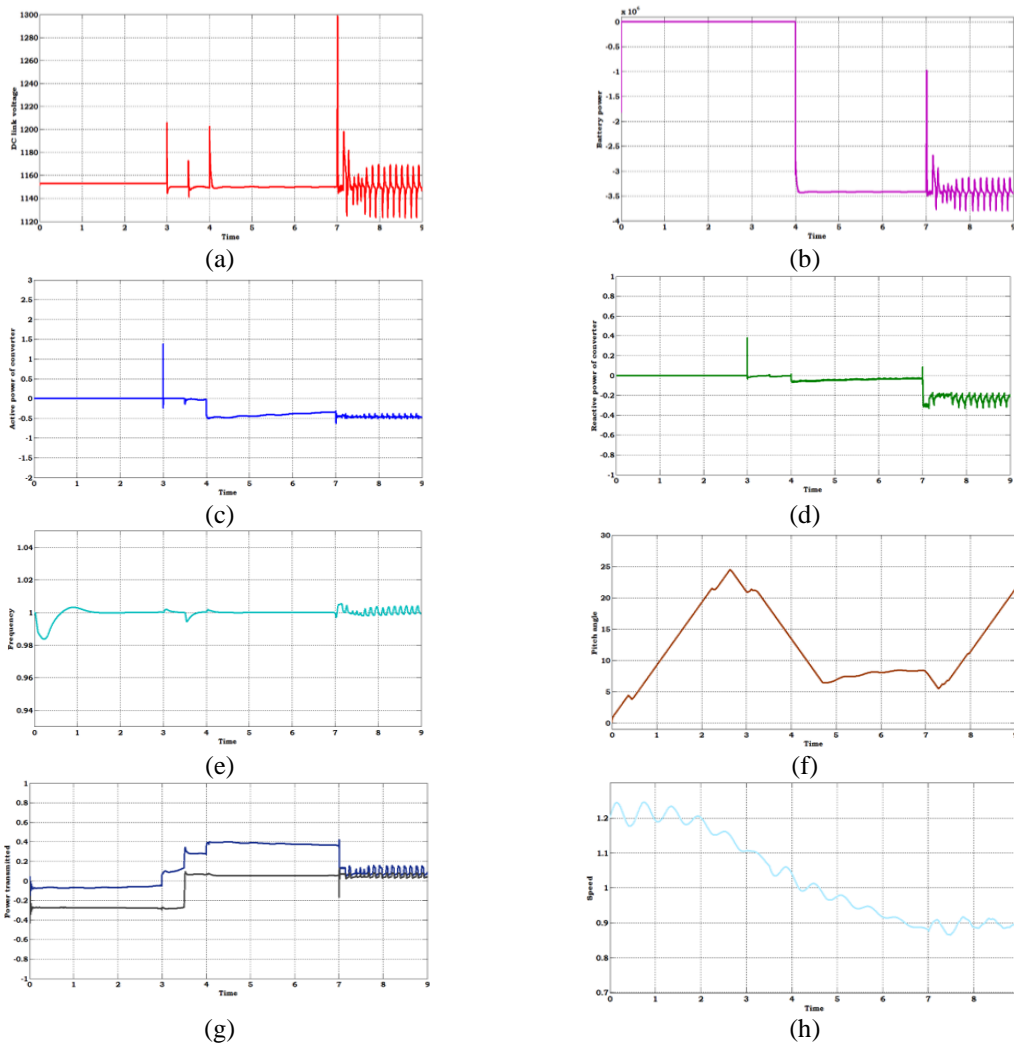


Figure 14. The waveforms of (a) voltage of the DC link, (b) power from a battery, (c) converter active power, (d) converter reactive power, (e) frequency, (f) angle of pitch, (g) transmission of power, and (h) when the OS is in islanded mode, the speed increases

**3.6. Test 6: when the OS is in islanded mode and more units are suddenly connected**

This mode is identical to the start-up scenario from t=0 to t=7 s, and at t=7 s, the same procedure of turning on certain loads was conducted as test 3. The waveforms of voltage of the DC link are shown in Figure 15(a). Battery power is shown in Figure 15(b). Frequency is shown in Figure 15(c) and speed when operating system in islanded mode with instant link of varying units is shown in Figure 15(d).

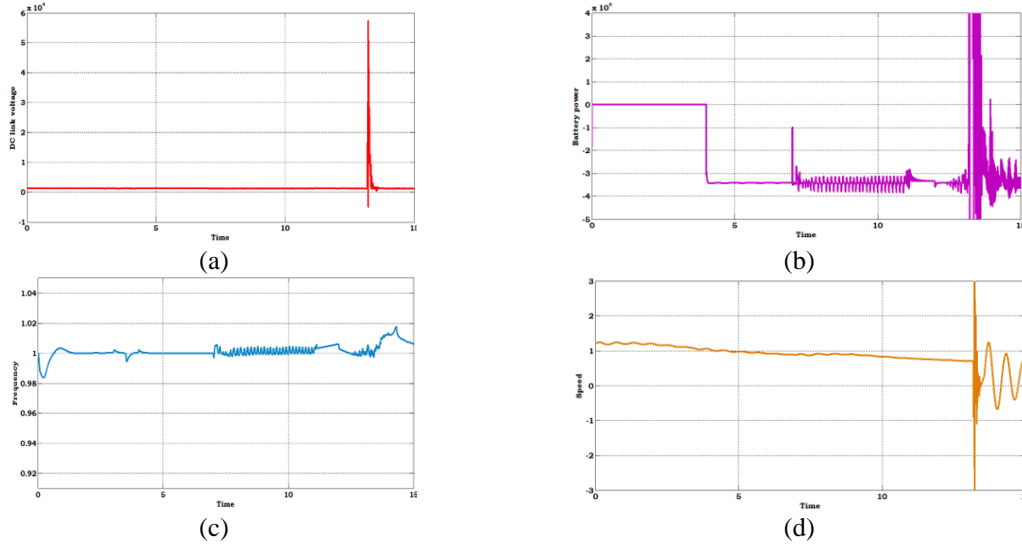


Figure 15. Waveforms of (a) DC voltage, (b) battery power, (c) frequency, and (d) speed when operating system in islanded mode with instant link of varying units

**3.7. Test 7: when the system is in islanded mode**

It is same as the start up case from t=0 s to t=7 s and at t=7 s, three phase fault has been created at point of common coupling and the same observations have been done as test 4. Waveforms of DC link voltage are shown in Figure 16(a). Frequency shown in Figure 16(b). Power generated is shown in Figure 16(c) and power transmitted when OS is in islanded mode with sudden fault is shown in Figure 16(d). From these tests (test 1 to 7), it can be concluded that for every disturbance that has been occurring in the proposed system, the controllers are continuously tracking the reference values to minimize the error and become stable. The setup of DFIG is shown in Table 1. The details regarding RL load is shown in Table 2. Induction generator specifications are shown in Table 3. Parameter values of the PV system are shown in Table 4.

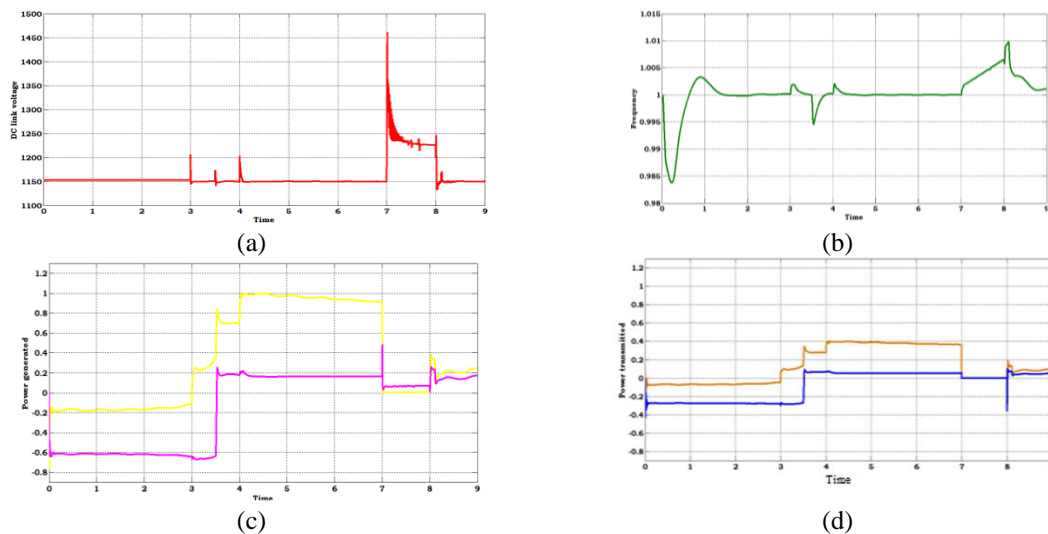


Figure 16. Waveforms of (a) DC link voltage, (b) frequency, (c) power generated, and (d) power transmitted when OS is in islanded mode with sudden fault

Table 1. The DFIG setup

S. No	Parameter	Value
1	DC Link voltage	1150 V
2	DC Link capacitor	1000 $\mu$ F
3	Wind velocity	10 m/s
4	Grid nominal voltage	120 KV
5	DFIG rated voltage	575 V

Table 2. Details regarding RL load

S. No	Parameters	Value
1	Active power	10e6
2	Inductive Reactive power	100e3
3	Capacitive Reactive Power	100e3
4	Nominal Voltage	25e3
5	Frequency	60 Hz

Table 3. Induction generator technical specifications

S. No	Parameter	Value
1	Purported current	6e6
2	Nominal voltage	575 V
3	Frequency	60 Hz

Table 4. Parameter values of the PV system

S. No	Parameter	Value
1	Nominal power	3730
2	Nominal voltage	460 V
3	Rated voltage of PV system	560 V

#### 4. CONCLUSION

This study demonstrates the creation of a renewable power apparatus that is contingent on an induction generator with the architecture of PI control technique DC voltage controller and direct torque regulator. The employed strategy enabled the system to functions efficiently in grid mode as well as islanded mode and also in parallel with other power generation units, loads, and FACTS devices. The analysis of different test cases in grid connected mode as well as islanded mode with PV generation unit, passive loads, induction motor loads, other wind power generation systems has been performed as test cases. The analysis of response of the system with the switching on and off of the other units has been performed and the results are verified using MATLAB 2013a.





#### REFERENCES

- [1] I. Boldea *et al.*, "Fractional kVA rating PWM converter doubly fed variable speed electric generator systems: an overview in 2020," *IEEE Access*, vol. 9, pp. 117957–117968, 2021, doi: 10.1109/ACCESS.2021.3101907.
- [2] A. Barkia, N. Bouchiba, S. Sallem, L. Chrifi-Alaoui, S. Drid, and M. B. A. Kammoun, "A comparative study of PI and Sliding mode controllers for autonomous wind energy conversion system based on DFIG," in *2016 17th International Conference on Sciences and Techniques of Automatic Control and Computer Engineering (STA)*, Dec. 2016, pp. 612–617. doi: 10.1109/STA.2016.7952039.
- [3] S. Li, "Converters' loading balance and stability verification for doubly-fed induction generator," *CSEE Journal of Power and Energy Systems*, 2022, doi: 10.17775/CSEEJPES.2021.01260.
- [4] P. P. Pradhan, B. Subudhi, and A. Ghosh, "A robust multiloop disturbance rejection controller for a doubly fed induction generator-based wind energy conversion system," *IEEE Journal of Emerging and Selected Topics in Power Electronics*, vol. 10, no. 5, pp. 6266–6273, Oct. 2022, doi: 10.1109/JESTPE.2022.3155561.
- [5] K. Naresh, P. Reddy, and P. Sujatha, "Design and comparison of performance of DFIG based wind turbine with PID controller, fuzzy controller, artificial neural network and model predictive controller," *EAI Endorsed Transactions on Energy Web*, vol. 9, no. 37, p. 170251, Jul. 2018, doi: 10.4108/eai.29-6-2021.170251.
- [6] M. A. Hossain and M. Bodson, "Control of a PMSM using the rotor-side converter of a doubly fed induction generator for hybrid-electric propulsion," *IEEE Transactions on Control Systems Technology*, vol. 30, no. 4, pp. 1758–1765, Jul. 2022, doi: 10.1109/TCST.2021.3113885.
- [7] Y. Zhang, J. Liu, M. Zhou, C. Li, and Y. Lv, "Double impedance-substitution control of DFIG based wind energy conversion system," *Energies*, vol. 15, no. 15, p. 5739, Aug. 2022, doi: 10.3390/en15155739.
- [8] R. Kosuru, S. Liu, and W. Shi, "Deep reinforcement learning for stability enhancement of a variable wind speed DFIG system," *Actuators*, vol. 11, no. 7, Jul. 2022, doi: 10.3390/act11070203.
- [9] W. Aicha, E. Abdelhadi, and S. R. Kaoutar, "Use of a doubly-fed induction generator for the conversion of wind energy," in *Digital Technologies and Applications*, S. Motahhir and B. Bossoufi, Eds. Cham, Switzerland: Springer, 2021, pp. 1245–1253. doi: 10.1007/978-3-030-73882-2\_114.
- [10] K. Tamvada and S. Umashankar, "Fuzzy rotor side converter control of doubly fed induction generator," in *Artificial Intelligence and Evolutionary Computations in Engineering Systems*, S. Dash, P. Naidu, R. Bayindir, and S. Das, Eds. Singapore: Springer, 2018, pp. 657–663. doi: 10.1007/978-981-10-7868-2\_62.
- [11] B. Abdesselam, B. Cherif, and B. Othmane, "Direct and indirect nonlinear control power of a doubly-fed-induction generator for wind conversion system under disturbance estimation," in *Smart Energy Empowerment in Smart and Resilient Cities*, M. Hatti, Ed. Cham, Switzerland: Springer, 2020, pp. 212–219. doi: 10.1007/978-3-030-37207-1\_22.
- [12] Z. Zeghdi, L. Barazane, A. Larabi, B. Benchama, and K. Khechiba, "Wind energy conversion systems based on a doubly fed induction generator using artificial fuzzy logic control," in *Renewable Energy for Smart and Sustainable Cities*, M. Hatti, Ed. Cham, Switzerland: Springer, 2019, pp. 255–262. doi: 10.1007/978-3-030-04789-4\_28.
- [13] K. Naresh, P. U. Reddy, P. Sujatha, and C. R. Reddy, "Control of DFIG based wind turbine with hybrid controllers," *International Journal of Renewable Energy Research*, vol. 10, no. 3, pp. 1488–1500, 2020.
- [14] A. Dida and D. Ben Attous, "Doubly-fed induction generator drive based WECS using fuzzy logic controller," *Frontiers in Energy*, vol. 9, no. 3, pp. 272–281, Sep. 2015, doi: 10.1007/s11708-015-0363-9.
- [15] C. Chhabra, K. Tharani, S. Banerjee, A. Verma, M. Bhatia, and S. Sethi, "Grid integration of doubly-fed induction machine using indirect field oriented control," *Journal of Information and Optimization Sciences*, vol. 43, no. 1, pp. 219–223, Jan. 2022, doi: 10.1080/02522667.2022.2039473.
- [16] S. Banerjee, D. Joshi, and M. Singh, "Mathematical modelling of doubly-fed induction generator," *Journal of Interdisciplinary*





- Mathematics*, vol. 23, no. 5, pp. 927–934, Jul. 2020, doi: 10.1080/09720502.2020.1723922.
- [17] Y. Ling, “A fault ride through scheme for doubly fed induction generator wind turbine,” *Australian Journal of Electrical and Electronics Engineering*, vol. 15, no. 3, pp. 71–79, Jul. 2018, doi: 10.1080/1448837X.2018.1525172.
- [18] S. Sharma and V. K. Tayal, “Optimised controller design for frequency control of a wind turbine driven doubly fed induction generator,” *International Journal of Ambient Energy*, vol. 43, no. 1, pp. 7197–7206, Dec. 2022, doi: 10.1080/01430750.2022.2063176.
- [19] M. S. Nazir and W. Qi, “Impact of symmetrical short-circuit fault on doubly-fed induction generator controller,” *International Journal of Electronics*, vol. 107, no. 12, pp. 2028–2043, Dec. 2020, doi: 10.1080/00207217.2020.1756447.
- [20] P. Verma, S. K. and B. Dwivedi, “Comprehensive investigation on doubly fed induction generator-Wind farms at fault ride through capabilities: technical difficulties and improvisations,” *Energy Sources, Part A: Recovery, Utilization, and Environmental Effects*, pp. 1–33, Jan. 2021, doi: 10.1080/15567036.2020.1857476.
- [21] C.-S. Tu, C.-M. Hong, and K.-H. Lu, “Design of novel intelligent controller for doubly-fed induction generator-driven wind turbine to improve transient control performance,” *Electric Power Components and Systems*, vol. 48, no. 1–2, pp. 174–185, Jan. 2020, doi: 10.1080/15325008.2020.1732503.
- [22] K. Naresh, P. U. Reddy, and P. Sujatha, “Analysis and performance comparison of multimode control scheme based doubly fed induction generator wind power unit with PMSG wind power unit,” *Journal of Green Engineering (JGE)*, vol. 10, no. 10, pp. 9328–9347, 2020.
- [23] P. Dahiya, V. Sharma, and R. N. Sharma, “Optimal generation control of interconnected power system including DFIG-based wind turbine,” *IETE Journal of Research*, vol. 61, no. 3, pp. 285–299, May 2015, doi: 10.1080/03772063.2015.1019579.
- [24] R. Yawata *et al.*, “A study on frequency adjustment mechanism for wind turbine generation systems,” *Journal of International Council on Electrical Engineering*, vol. 9, no. 1, pp. 113–122, Jan. 2019, doi: 10.1080/22348972.2019.1706225.
- [25] E. E. C. Morais, F. K. de A. Lima, J. M. L. Fonseca, C. G. C. Branco, and L. de A. Machado, “Providing ancillary services with wind turbine generators based on DFIG with a two-branch static converter,” *Energies*, vol. 12, no. 13, Jun. 2019, doi: 10.3390/en12132490.
- [26] P. H. P. Silva, F. K. de A. Lima, J. M. L. Fonseca, C. G. C. Branco, and C. R. Schmidlin Júnior, “Synchronous compensator based on doubly fed induction generator to improve the power quality under unbalanced grid voltage conditions,” *Energies*, vol. 11, no. 10, Oct. 2018, doi: 10.3390/en11102803.
- [27] A. Parida and D. Chatterjee, “An improved control scheme for grid connected doubly fed induction generator considering wind-solar hybrid system,” *International Journal of Electrical Power & Energy Systems*, vol. 77, pp. 112–122, May 2016, doi: 10.1016/j.ijepes.2015.11.036.
- [28] P. Pura and G. Iwanski, “Direct torque control of a doubly fed induction generator working with unbalanced power grid,” *International Transactions on Electrical Energy Systems*, vol. 29, no. 4, Apr. 2019, doi: 10.1002/etep.2815.
- [29] G. Song, C. Zhang, X. Wang, and W. Huang, “Simplified method of doubly fed induction generator,” *The Journal of Engineering*, vol. 2017, no. 13, pp. 1200–1205, Jan. 2017, doi: 10.1049/joe.2017.0519.
- [30] K. Naresh, P. U. Reddy, and P. Sujatha, “Wind based doubly fed induction generator for effective rotor side converter control,” *International Journal of Innovative Technology and Exploring Engineering*, vol. 8, no. 9S3, pp. 273–278, Aug. 2019, doi: 10.35940/ijitee.I3050.0789S319.
- [31] H. Sita, P. U. Reddy, and R. Kiranmayi, “Optimal location and sizing of UPFC for optimal power flow in a deregulated power system using a hybrid algorithm,” *International Journal of Ambient Energy*, vol. 43, no. 1, pp. 1413–1419, Dec. 2022, doi: 10.1080/01430750.2019.1707116.
- [32] M. S. Giridhar, S. Sivanagaraju, C. V. Suresh, and P. Umapathi Reddy, “Analyzing the multi objective analytical aspects of distribution systems with multiple multi-type compensators using modified cuckoo search algorithm,” *International Journal of Parallel, Emergent and Distributed Systems*, vol. 32, no. 6, pp. 549–571, Nov. 2017, doi: 10.1080/17445760.2016.1173214.
- [33] Z. Le, W. Xueguang, K. Longze, L. Dong, L. Fangyuan, and H. Mingxiao, “Control strategy of doubly-fed induction generator during the grid voltage swell,” *The Journal of Engineering*, vol. 2019, no. 16, pp. 1807–1811, Mar. 2019, doi: 10.1049/joe.2018.8834.
- [34] H. Nian and X. Yi, “Coordinated control strategy for doubly-fed induction generator with DC connection topology,” *IET Renewable Power Generation*, vol. 9, no. 7, pp. 747–756, Sep. 2015, doi: 10.1049/iet-rpg.2014.0347.
- [35] B. Mansoor, P. Shashavali, and M. Khaimulla, “Implementation of droop control in doubly fed induction generator based wind turbines,” *International Journal of Advanced Research in Electrical, Electronics and Instrumentation Engineering*, vol. 5, no. 8, pp. 202–211, 2016.

## BIOGRAPHIES OF AUTHORS







**Kelothu Naresh**     presently Pursuing Ph.D. from JNTUA Ananthapuramu in EEE department and working as Associate Professor in department of Electrical and Electronics Engineering from Usha Rama College of Engineering and Technology. He has completed M. Tech from IIT Kharagpur in the Control Systems and completed B. Tech from VIIT in the branch of EEE. He has 16 international publications. His research areas include power systems, control systems, and renewable energy sources. He can be contacted at email: naresh5kelothu@gmail.com.



**Puthireddy Umapathi Reddy**     presently working as Professor in department of Electrical and Electronics Engineering from Sree Vidyanekithan Engineering College (Autonomous), Tirupati, Andhra Pradesh and has more than 23-years of teaching experience and 16 years research experience. He has published 28-international research papers. His research area includes power systems, control systems, and renewable energy sources. He can be contacted at email: [moni\\_uma@yahoo.co.in](mailto:moni_uma@yahoo.co.in).



**Peddakotla Sujatha**     presently working as Principal and Professor in department of Electrical and Electronics Engineering from JNTUA CEA Ananthapuramu and has more than 23 years teaching experience. She has published 48 international research papers. She involved major role for development of JNTUA CEA. Her research area includes power systems, control systems, and renewable energy sources. She can be contacted at email: [psujatha1993@gmail.com](mailto:psujatha1993@gmail.com).